Journal Pre-proof

Multifunctional cation-vacancy-rich $ZnCo_2O_4$ polysulfide-blocking layer for ultrahigh-loading Li-S battery

Zhenwei Li, Qian Zhang, Luke Hencz, Jie Liu, Payam Kaghazchi, Jishu Han, Lei Wang, Shanqing Zhang

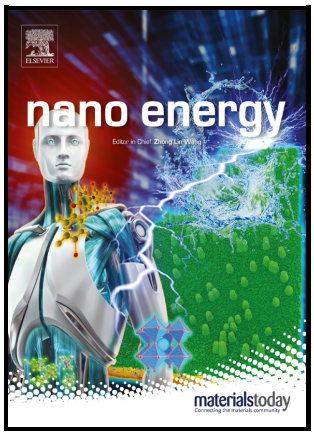

PII: S2211-2855(21)00586-3

DOI: https://doi.org/10.1016/j.nanoen.2021.106331

Reference: NANOEN106331

To appear in: *Nano Energy*

Received date: 28 May 2021
Revised date: 7 July 2021
Accepted date: 7 July 2021

Please cite this article as: Zhenwei Li, Qian Zhang, Luke Hencz, Jie Liu, Payam Kaghazchi, Jishu Han, Lei Wang and Shanqing Zhang, Multifunctional cation-vacancy-rich $ZnCo_2O_4$ polysulfide-blocking layer for ultrahigh-loading Li-S battery, *Nano Energy,* (2021) doi:https://doi.org/10.1016/j.nanoen.2021.106331

Multifunctional cation-vacancy-rich $ZnCo_2O_4$ polysulfide-blocking layer for ultrahigh-loading Li-S battery

Zhenwei Li[a,c,1], Qian Zhang[a,c,1], Luke Hencz[d,1], Jie Liu[a,b*], Payam Kaghazchi[e], Jishu Han[a,c], Lei Wang[a,f*], Shanqing Zhang[d*]

[a]*State Key Laboratory Base of Eco-chemical Engineering, Taishan Scholar Advantage and Characteristic Discipline Team of Eco-chemical Process and Technology, Qingdao University of Science and Technology, Qingdao 266042, China. Email: jie.liu@qust.edu.cn (J. Liu), inorchemwl@126.com (L. Wang)*

[b]*College of Chemical Engineering, Qingdao University of Science and Technology, Qingdao 266042, China*

[c]*College of Chemistry and Molecular Engineering, Qingdao University of Science and Technology, Qingdao 266042, China*

[d]*Centre for Clean Environment and Energy, School of Environment and Science, Gold Coast Campus, Griffith University, QLD 4222, Australia. Email: s.zhang@griffith.edu.au (S. Zhang)*

[e]*Institute of Energy and Climate Research, Forschungszentrum Jülich GmbH, Jülich 52425, Germany*

[f]*Shandong Engineering Research Center for Marine Environment Corrosion and Safety Protection, College of Environment and Safety Engineering, Qingdao University of Science and Technology, Qingdao 266042, China.*

[1]*These authors contributed equally.*

Abstract: The major hurdle in Li-S battery commercialization is the severe shuttle effect and sluggish reaction kinetics of polysulfide conversion during charge-discharge cycling. Herein, to overcome these barriers, we designed and synthesized Zn defective Zn/Co oxide (ZDZCO) nanosheets, a cation-vacancy-rich bimetallic oxide for the construction of a multifunctional polysulfide-blocking layer. Both theoretical and experimental studies have comprehensively demonstrated that the ZDZCO shows robust binding capability towards polysulfides and a high catalytic ability for fast polysulfide conversion. Through a facile coating process, the multifunctional ZDZCO polysulfide-blocking layer is incorporated on a commercial polypropylene separator, forming a composite separator. The resultant separator facilitates an ultrahigh sulfur loading of 21.06 mg cm^{-2} and an areal capacity as high as 24.25 mAh cm^{-2}. This study illuminates a promising and practical strategy to construct high-performance Li-S batteries with high sulfur loading.

Graphical Abstract

A multifunctional cation-vacancy-rich $ZnCo_2O_4$ modified separator has been developed to create a strong affinity to polysulfides and rapid catalytic conversion between the polysulfides for the achievement of ultrahigh areal loading and high-performance Li-S batteries.

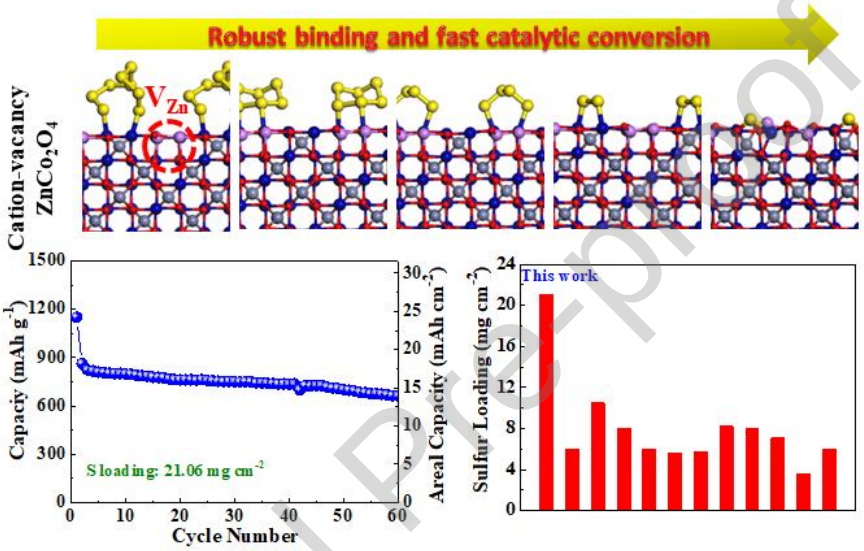

Keywords: multifunctional separator; ultrahigh loading; cation vacancy; strong affinity; high catalytic ability

1. Introduction

Owing to the advantages of high energy density (2600 Wh kg^{-1}), low cost, and eco-friendliness, the Li-S battery is considered as one of the most promising energy storage devices for electric vehicles, hybrid electric vehicles, and smart power grids [1-3]. However, the electrochemical performance of Li-S batteries is severely restricted by the poor electronic

conductivity of the active sulfur material and its discharge products (Li_2S_2/Li_2S), the large volume expansion associated with the conversion of sulfur to Li_2S_2/Li_2S, and the notorious shuttle effect of soluble polysulfides (Li_2S_x, $4 \leq x \leq 8$) [4,5]. The intractable shuttle effect is especially troublesome, as it leads to fast active material loss, low columbic efficiency, and severe corrosion and passivation of the Li anode, resulting in rapid electrochemical performance degradation [6-8].

Despite this, through the rational design of polysulfide host materials, high-performance Li-S batteries have been achieved. Various carbonaceous materials [9-11], functional polymers [12-15], and metal compounds [16-20] have been constructed and applied as host materials to improve the electrochemical performance of Li-S batteries. In addition to being applied to prepare S/host material composites, which are capable of immobilizing polysulfides in the cathode matrix, polysulfide-anchoring materials can also be applied in the construction of functional composite separators to effectively deliver a polysulfide shuttle barrier. Usually, when the anchoring materials are applied to modify the separator, rather than as cathodic polysulfide hosts, less inactive anchoring materials are used, which improves the gravimetric energy density of the whole cell and aligns with the goal of a high-energy-density Li-S battery. Up to now, extensive efforts have been devoted to modifying commercial separators so that the cycling performance of Li-S batteries can be enhanced [21-32]. For example, an ion-selective Nafion-based layer modified Celgard separator was constructed to confine the polysulfide anions at the cathode side via the shielding effect [21,22]. Alternatively, with the advantage of high electronic conductivity, a nonpolar super P-modified separator can function as both an upper current collector and a polysulfide-diffusion barrier by physical blocking [23,26]. In contrast to physically blocking polysulfide migration, polar materials such as heteroatom-doped carbons,

functional polymers, and metal compounds can immobilize polysulfides via strong chemical adsorption, which builds a more effective polysulfide-blocking layer on the separators [25,27,29,31,32].

Although the cycling stability and discharge capacity of Li-S batteries have been significantly enhanced through the application of functional separators, most of the previous separator-related research is based on batteries with low sulfur loading, which cannot satisfy the high energy density required for practical applications. To obtain a sufficient energy density, it is crucial to fabricate high-loading Li-S batteries that can deliver a high areal capacity [33,34]. It has been reported that a sulfur loading of > 5 mg cm^{-2} with a specific capacity of 1000 mAh g^{-1}, corresponding to an areal capacity of 5 mAh cm^{-2}, is required to achieve a satisfactorily high energy density by Li-S battery [35]. However, as the sulfur loading increases, so too does the severity of polysulfide dissolution and shuttling, making it very difficult to simultaneously achieve a high-loading Li-S battery with high performance. Even though strong-affinity materials on separators can effectively immobilize polysulfides, the sluggish reaction kinetics of polysulfide conversion results in the chronic occupation of the adsorption sites on the functional materials, leading to reduced polysulfide affinity after prolonged cycling. Recently, it has been demonstrated that the introduction of catalytic functionality into high-affinity functional materials is an efficient and promising strategy to achieve fast polysulfide conversion [36-41]. Vast efforts have been devoted to constructing catalytic cathodes, while the development of catalytic separators is still in the early stage. Considering the reduced dosage of anchoring materials in functional separators, significantly enhanced catalytic properties are required if a high-performance Li-S battery is to be achieved, especially in the case of high sulfur loading.

Therefore, the great challenge of designing robust-affinity and highly-catalytic functional material modified separators for high-loading Li-S batteries with high performance still remains.

Constructing defects into functional materials has been demonstrated as a highly effective approach to boost the catalytic abilities and polysulfide affinity of functional materials for Li-S batteries [41,42]. Amongst these, anion vacancies are usually constructed to achieve high-performance functional materials [43-45]. While, to the best of our knowledge, cation vacancies are rarely studied. Herein, a new anchoring functional material design strategy has been proposed via cation vacancies for high-loading Li-S batteries. Co_3O_4, a strong-affinity host material for polysulfides [46], was chosen as a model to prove our new anchoring functional material design strategy. By partly replacing Co with Zn and in-situ etching, Zn defective $ZnCo_2O_4$ (ZDZCO) nanosheets were prepared to achieve the Zn vacancies. Both theoretical and experimental studies have demonstrated that the ZDZCO possesses robust binding capability towards polysulfides and a high catalytic ability for polysulfide conversion, resulting from the cation vacancies. As a result, when the ZDZCO was applied in the construction of a novel multifunctional polysulfide-blocking layer on a commercial separator, Li-S battery with an ultrahigh loading of 21.06 mg cm^{-2} can be achieved, which is stable over 60 cycles and delivers a high areal capacity of 13.95 mAh cm^{-2}. To the best of our knowledge, such a cycling lifespan of a Li-S battery with ultrahigh loading prepared via traditional electrode preparation technique has rarely been reported.

2. Results and discussion

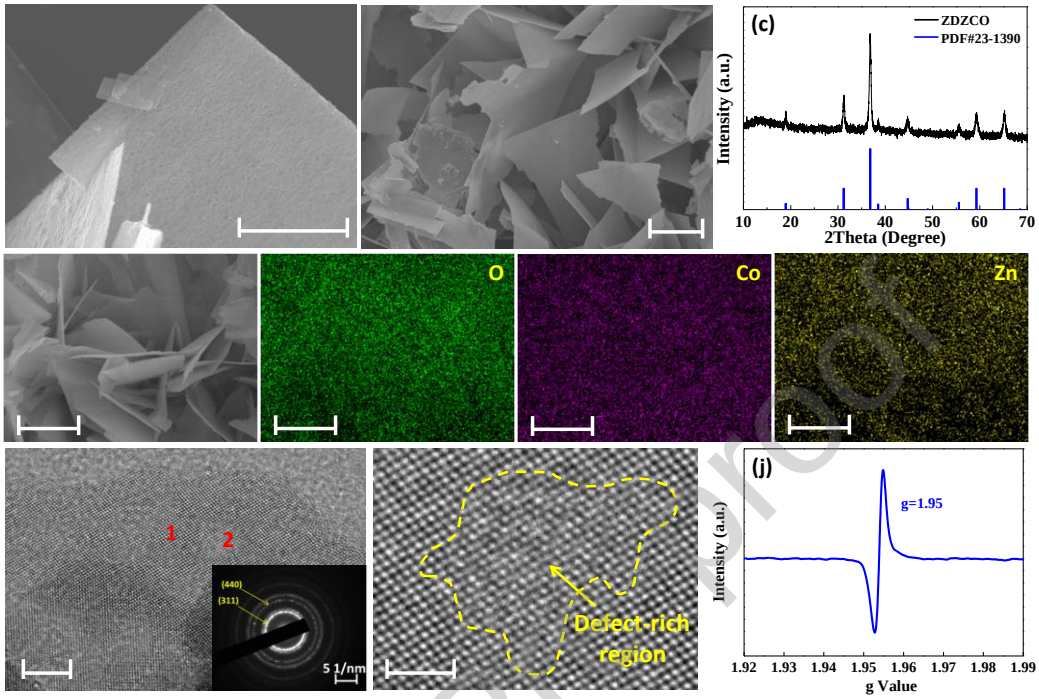

Figure 1. (a, b) SEM images and (c) XRD pattern of as-prepared ZDZCO; (e-g) O, Co, and Zn element distribution in the ZDZCO in (d); (h) TEM image of as-prepared ZDZCO and (i) corresponding enlarged view of section 2; (j) EPR spectrum of as-prepared ZDZCO. The inset in (h) is the SAED pattern of as-prepared ZDZCO.

Normally, in strong alkaline solutions at room temperature, Zn^{2+} in the solid-phase can react with OH^- to form soluble $Zn(OH)_4^{2-}$, leading to Zn vacancies [47]. This work, in contrast to the referenced work, partly replaces the Co in Co_3O_4 with Zn and etches the Zn in-situ in the presence of urea during a facile hydrothermal method. The hydrolysis of urea offers mild alkaline conditions and active NH_3 ligands to react with Zn^{2+} and achieve Zn vacancies in $ZnCo_2O_4$, resulting in the Zn-deficient Zn/Co oxide (ZDZCO). The as-prepared ZDZCO is large-area thin 2D nanosheets with some aggregation occurring, as indicated by the SEM images in Fig. 1a, b and S1. The XRD pattern of the obtained ZDZCO (Fig. 1c) shows diffraction peaks at 2θ =

18.97°, 31.26°, 36.79°, 38.51°, 44.84°, 55.54°, 59.33°, and 65.20°, which are assigned to (111), (220), (311), (222), (400), (422), (511), and (440) crystal planes of spinel $ZnCo_2O_4$ phase (PDF No. 23-1390). The ratio of Zn and Co in the ZDZCO nanosheets, as determined by ICP-OES analysis, is 0.87:2, leading to a formula of $Zn_{0.87}Co_2O_4$. The element mappings (Fig. 1e-g) of the ZDZCO nanosheets in Fig. 1d demonstrate that the Co, Zn, and O elements are distributed uniformly. From the HRTEM images in Fig. S2 (enlarged view of section 1 in Fig. 1h), one can clearly observe an interplanar spacing of 0.27 nm, which is assigned to the (220) plane of $ZnCo_2O_4$, with the SAED patterns (inset in Fig. 1h) also showing the diffraction rings of (311) and (440) planes of $ZnCo_2O_4$. In Fig. 1i (enlarged view of section 2 in Fig. 1h), numerous small pits on the surface of the as-prepared ZDZCO can be obviously observed, visually indicating the presence of defects in the ZDZCO nanosheets. Moreover, the as-prepared ZDZCO shows a strong EPR signal at g=1.95 (Fig. 1j), clearly indicating a large amount of Zn vacancies [48]. As a control, the Co_3O_4 nanosheets are synthesized through the same process without adding $Zn(NO_3)_2 \cdot 6H_2O$ (Fig. S3).

To prepare the ZDZCO polysulfide-blocking layer modified separator (ZDZCO-separator), the ZDZCO-based composite is coated on a commercial PP separator using a blade coating method with ZDZCO nanosheets, super P, and PVDF binder in a mass ratio of 6:3:1. The loading of the coating was controlled to be about 0.28 mg cm^{-2}. Super P was included in the ZDZCO-separator as a conductive additive to allow the modified separator to function as an upper current collector. The integrity of the as-prepared ZDZCO separator after folding, displayed in Fig. 2a, indicates good adhesion between ZDZCO polysulfide-blocking layer and PP separator. The thickness of the ZDZCO polysulfide-blocking layer is measured to be 2.4 μm, as shown in the cross-section SEM image of the ZDZCO-separator (Fig. 2b). For comparison, a

super P-separator was also prepared with super P and PVDF binder in a mass ratio of 9:1. Fig. 2c shows that with the same mass loading level, the super P coating layer shows a much larger thickness (11.0 μm), which is almost 5 times thicker than the ZDZCO polysulfide-blocking layer. As a consequence, higher volumetric energy density can be achieved using ZDZCO-separator. By comparing the top-view SEM image of the ZDZCO-separator and super P-separator displayed in Fig. 2d and S4, one can observe that the ZDZCO nanosheets are uniformly embedded in the super P conductive carbon matrix. The element mappings (Fig. 2e-g) obviously show that the Zn, Co, and C elements are dispersed over the separator. As a consequence, it is expected that the ZDZCO-separator can not only effectively immobilize polysulfides but also act as an upper current collector for the continual conversion of polysulfides.

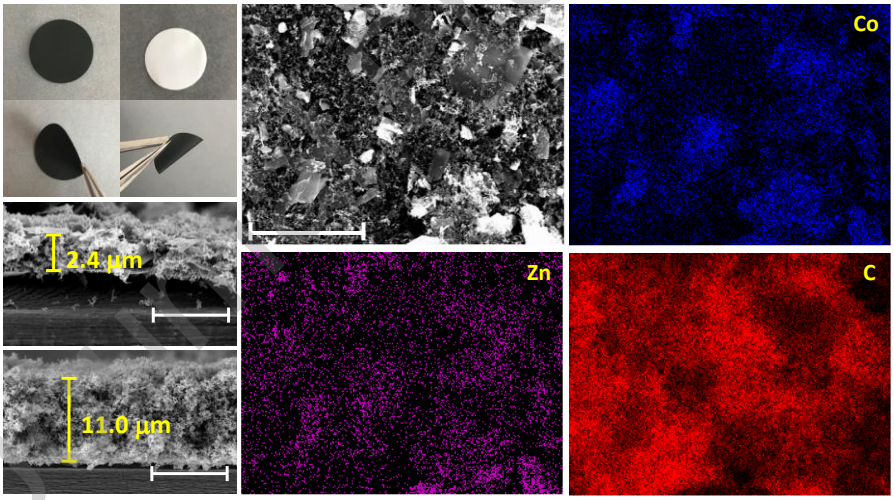

Figure 2. (a) Digital photos of as-prepared ZDZCO-separator; cross-section SEM images of (b) ZDZCO-separator and (c) super P-separator; (d) top-view SEM image and (e-g) element mappings of the ZDZCO-separator.

Electrochemical tests were carried out at room temperature to evaluate the effect of the ZDZCO-separator on the cycling performance of Li-S batteries. Firstly, the electrochemical

activity of ZDZCO between 1.8 and 2.6 V was studied through CV and charge-discharge cycling tests. As shown in Fig. S6, the ZDZCO is inactive and contributes negligible capacity between 1.8 and 2.6 V. The sulfur cathode was prepared with 80 wt% S/super P composite, 10 wt% Ketjen black (KB), and 10 wt% PVDF binder. It should be noted that in the sulfur cathode, there are no additional polysulfide hosts. Fig. 3a shows the typical charge-discharge behavior of a Li-S battery, i.e., the formation of long-chain polysulfides (Li_2S_x, $4 \leq x \leq 8$) at 2.31 V and the conversion of Li_2S_x to Li_2S_2/Li_2S at 2.03 V [49]. The charge-discharge curves (Fig. 3b) also display the typical two-platform discharge behaviour which is characteristic of the Li-S battery. The cycling stability of the Li-S batteries with different separators at 0.5 C after an initial cycle at 0.2 C is compared in Fig. 3c. It indicates that the Li-S battery with ZDZCO-separator shows superior cycling stability with a high capacity of 857 mAh g^{-1} after 125 cycles, which is higher than that of Li-S battery with PP separator (547 mAh g^{-1}), super P-separator (703 mAh g^{-1}), and Co_3O_4-separator (771 mAh g^{-1}). Moreover, as shown in Fig. 3d and S5, the Li-S battery with ZDZCO-separator also shows superior rate properties, delivering a high capacity of 731 mAh g^{-1} at 6.0 C. The long-term cycling performance of the Li-S battery with the ZDZCO-separator at high current density of 2.0 C is displayed in Fig. 3e. It shows that the Li-S battery can still deliver a high capacity of 557 mAh g^{-1} after 450 cycles, indicating high long-term cycling stability. Furthermore, the Li-S battery displays a high coulombic efficiency of 99.8% after 450 cycles, suggesting suppressed shuttle effect. To further show the effectiveness of the ZDZCO-separator at suppressing the polysulfide shuttle, an electrolyte without $LiNO_3$ additive is applied. A $LiNO_3$ additive is known to promote the formation of a stable passivation film on the Li anode, which can significantly suppress the polysulfide shuttle [50], thus, by cycling a cell without the $LiNO_3$ additive, the role of the ZDZCO-separator is highlighted. As shown in Fig. 3f, the Li-S

battery with ZDZCO-separator can still give a stable and high capacity of 691 mAh g^{-1} with a high coulombic efficiency of 95.8% after 100 cycles even without the $LiNO_3$ additive. Even when the ZDZCO-coating loading is decreased to 0.16 mg cm^{-2}, the Li-S battery with ZDZCO-separator can also show high cycling stability with a capacity of 754 mAh g^{-1} and coulombic efficiency of 99.9 % after 150 cycles (Fig. 3g). These excellent electrochemical performances have comprehensively demonstrated that the ZDZCO-separator possesses great application potential for high-performance Li-S batteries.

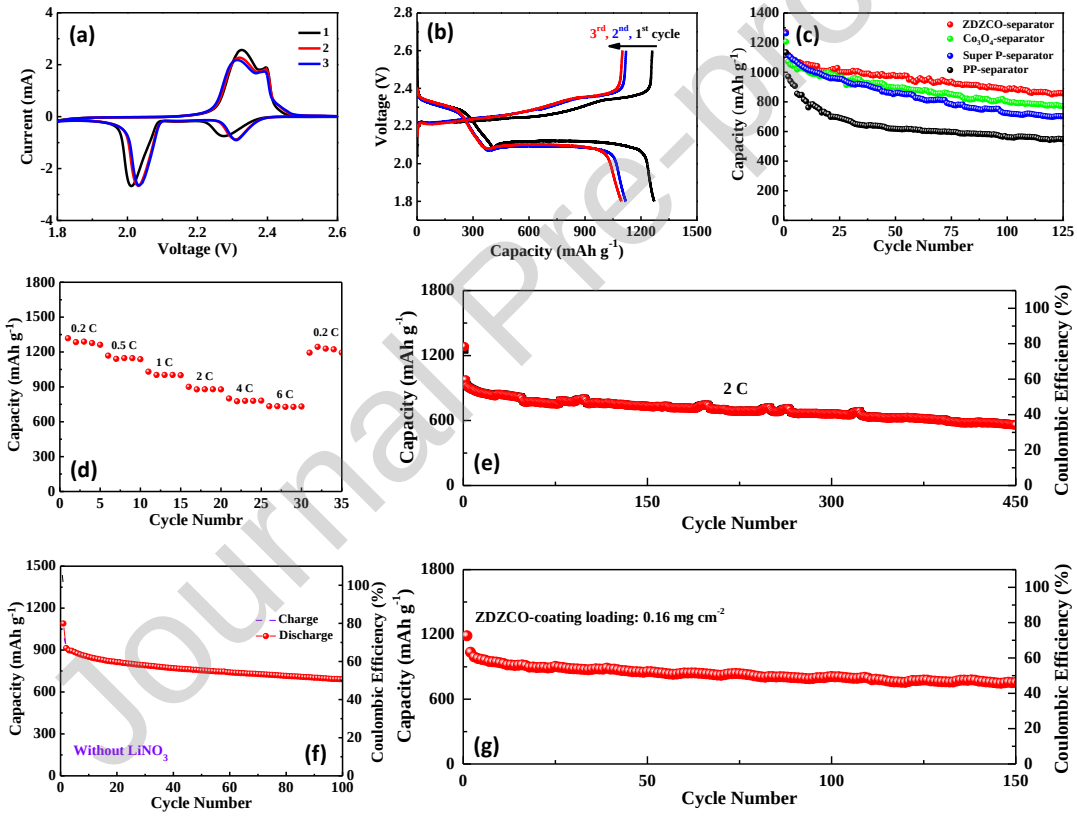

Figure 3. (a) CV curves and (b) charge-discharge curves of Li-S batteries with ZDZCO-separators; (c) comparison of cycling stability of Li-S batteries with different separators; (d) rate property and (e) long-term cycling performance at a high current density of 2 C of Li-S batteries with ZDZCO-separators; cycling performance of Li-S batteries with ZDZCO-separators (f)

without $LiNO_3$ additive and (g) under a low ZDZCO-coating loading of 0.16 mg cm^{-2} with $LiNO_3$ additive.

To deeply understand the reasoning behind the enhanced electrochemical performance of Li-S batteries with ZDZCO-separator, a series of theoretical and experimental studies were carried out. Density functional theory (DFT) calculations have proven themselves as a powerful and widely applied way to study the binding energy (BE) of host materials with polysulfides, often to explain an enhanced electrochemical performance obtained experimentally. Herein, to analyze the anchoring capability of the functional material towards polysulfide molecules, we calculated the BE between polysulfide molecules and the (100) surface of Co_3O_4, $ZnCo_2O_4$, and $Zn_{0.875}Co_2O_4$. The most favorable atomic configurations of sulfur species (*i.e.*, S_8, Li_2S_8, Li_2S_6, Li_2S_4, Li_2S_2, and Li_2S) anchored on (100) surface of Co_3O_4, $ZnCo_2O_4$, and $Zn_{0.875}Co_2O_4$ and the calculated BEs are shown in Fig. 4. It is found that $Zn_{0.875}Co_2O_4$ offers the strongest BEs with Li_2S_x (-5.72, -6.42, -5.34, -6.72, and -9.45 eV for Li_2S_8, Li_2S_6, Li_2S_4, Li_2S_2, and Li_2S, respectively). Moreover, the BEs between $ZnCo_2O_4$ and Li_2S_x (-4.92, -4.79, -3.87, -5.65, and -6.41 eV for Li_2S_8, Li_2S_6, Li_2S_4, Li_2S_2, and Li_2S, respectively) are slightly stronger than those between Co_3O_4 and Li_2S_x (-4.75, -4.73, -3.62, -5.12, and -5.76 eV for Li_2S_8, Li_2S_6, Li_2S_4, Li_2S_2, and Li_2S, respectively). In our calculations, van der Waals interactions were also considered to correctly calculate the adsorption energy. When the Li_2S_8 molecule is reduced to Li_2S_6 a decrease in the distance between the $Zn_{0.875}Co_2O_4$ surface and the respective polysulfide occurs, which can explain the increased adsorption energy displayed between Li_2S_6 and $Zn_{0.875}Co_2O_4$, as shown in Fig. S7. It is noteworthy that Li ions from Li_2S_x ($2 \leq x \leq 8$) prefer to bind to oxygen anions in the top layer of the surface. Simultaneously, polysulfide ions are bonded to two adjacent octahedral Co cations in the top layer of all three systems. Interestingly, a surface

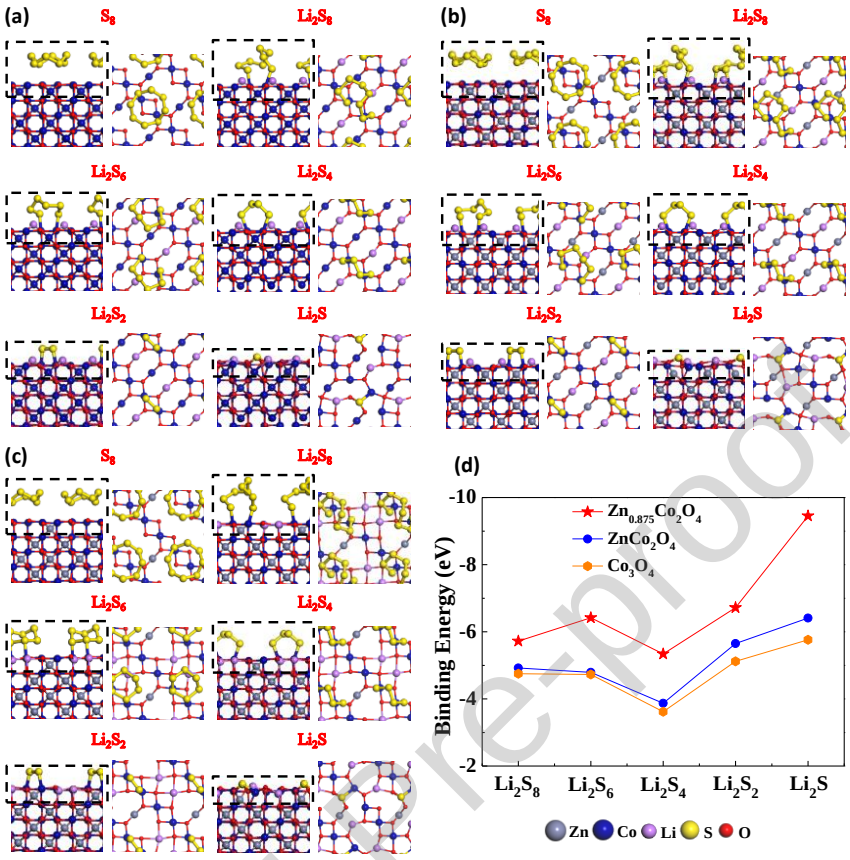

Figure 4. Atomic configurations for the sulfur species (*i.e.*, S_8, Li_2S_8, Li_2S_6, Li_2S_4, Li_2S_2, and Li_2S) adsorbed on the (100) surface of (a) Co_3O_4, (b) $ZnCo_2O_4$, and (c) $Zn_{0.875}Co_2O_4$; (d) the corresponding binding energies between the sulfur species and Co_3O_4(100), $ZnCo_2O_4$(100), and $Zn_{0.875}Co_2O_4$(100).

rearrangement arises when a Li_2S molecule adsorbs on the (100) surface of all three systems. The Li_2S molecule inserts in the top layer of the surface structure and causes one Co atom to diverge from the octahedral site. In this case, S^{2-} binds to two oxygen anions and one Co cation in the top layer, which results in a much stronger BE between Li_2S and the surfaces compared with other sulfur species. The significantly enhanced BEs between Li_2S_x and $Zn_{0.875}Co_2O_4$ is due to the insertion of Li ions into the subsurface layers of $Zn_{0.875}Co_2O_4$ surface. The Zn vacancy in the subsurface layer provides enough space for a Li-ion to penetrate into the surface and binds more

strongly to oxygen anions in the top layer. These DFT results obviously suggest that constructing cation vacancies is an efficient and promising way to design strong-affinity anchoring functional materials for Li-S batteries.

To experimentally indicate the strong affinity of ZDZCO towards polysulfides, polysulfide adsorption tests were performed. Initially, the Li_2S_6 solution is deep yellow (inset in Fig. 5a); however, after adding ZDZCO nanosheets and standing for about 48h, the solution becomes almost colorless, suggesting that most of the polysulfides are adsorbed on the ZDZCO surfaces. Conversely, the solutions with Co_3O_4 and super P still retain their yellow colour, suggesting a large amount of free Li_2S_6 still exists in the solutions. The UV-visible absorption spectra shown in Fig.5a quantitatively compare the Li_2S_6 remnant in the solutions after the adsorption tests. It shows that the ZDZCO has the strongest affinity towards polysulfides, as the remnant Li_2S_6 in the solution with ZDZCO is the lowest. H-shaped glass cells are set up to show the polysulfide blocking capability of the ZDZCO-separator (Fig. 5b and S8). Half of the glass cell (left) was filled with 50 mL of 4 mmol L^{-1} Li_2S_6 solution and the other half (right) was filled with 50 mL of tetrahydrofuran (THF), and separated by a PP separator, super P-separator, Co_3O_4-separator, and ZDZCO-separator, respectively. From Fig. S8, one can observe that the right chambers rapidly change to yellow after several hours, suggesting Li_2S_6 can easily diffuse across the PP separator, super P-separator, and Co_3O_4-separator. Conversely, in the cell containing the ZDZCO separator, the polysulfides are contained in the left chamber, while the right chamber remains colourless (Fig. 5b and S8) owing to the strong polysulfide restriction ability of ZDZCO. As a consequence, in a Li-S cell, the Li anode can retain a smooth morphology, almost without Li_2S deposition when the ZDZCO-separator is applied (Fig. S9) [39,51].

In order to further understand the chemical adsorption interaction between ZDZCO and polysulfides, X-ray photoelectron spectroscopy (XPS) spectra of ZDZCO before and after adsorbing polysulfides (Li_2S_6) are compared. For the pristine ZDZCO, the high-resolution Co 2p spectrum in Fig. 5c displays peaks at the binding energies of 780.87 and 796.31 eV, which are associated with Co $2p_{3/2}$ and Co $2p_{1/2}$ of Co^{2+}, and peaks at 779.55 and 794.65 eV, which are associated with Co $2p_{3/2}$ and Co $2p_{1/2}$ of Co^{3+}, suggesting the coexistence of Co(II) and Co(III) [52-54]. In the high-resolution Zn 2p spectrum (Fig. 5e), two peaks are located at binding energies of 1020.67 and 1043.77 eV, attributed to Zn $2p_{3/2}$ and Zn $2p_{1/2}$, indicating the Zn(II)

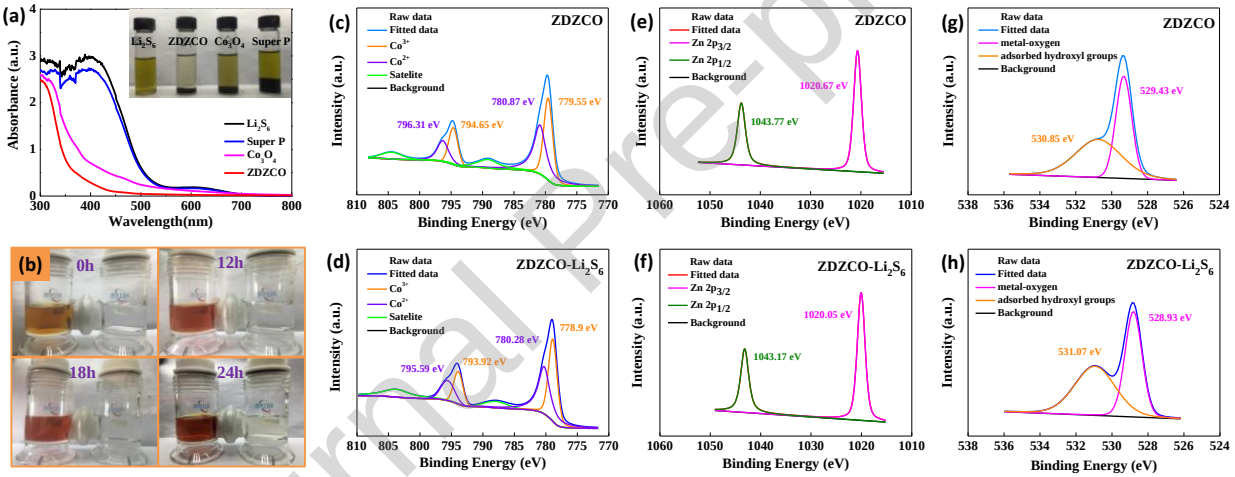

Figure 5. (a) UV-visible spectra of the Li_2S_6 solution after polysulfide adsorption tests (inset is the photo of the Li_2S_6 solutions after polysulfide adsorption tests); (b) the photos of the polysulfide diffusion experiment using ZDZCO-separator; high-resolution XPS spectra of (c) Co 2p, (e) Zn 2p, and (g) O 1s for ZDZCO, and (d) Co 2p, (f) Zn 2p, and (h) O 1s for ZDZCO adsorbing Li_2S_6, respectively.

oxidation state. The O 1s XPS spectrum in Fig. 5g shows a peak at 529.43 eV that can be assigned to metal-oxygen bonding in ZDZCO with the peak at 530.85 eV attributed to the oxygen of surface adsorbed hydroxyl groups [54]. After adsorbing Li_2S_6, Fig 5d and f display

that, overall, the major peaks corresponding to Co 2p and Zn 2p obviously shift to lower binding energies, ascribed to the electron transfer from polysulfides to the metal atoms, indicating that a strong chemical interaction occurs [55,56]. Similarly, the peak for metal-oxygen bonding in the O 1s spectrum (Fig. 5h) also shifts to lower binding energy after interacting with Li_2S_6, due to the strong chemisorption between ZDZCO and Li_2S_6. The above results comprehensively justify that the first mechanism by which the ZDZCO-separator improves the cycling performance of Li-S batteries is through its robust polysulfide affinity.

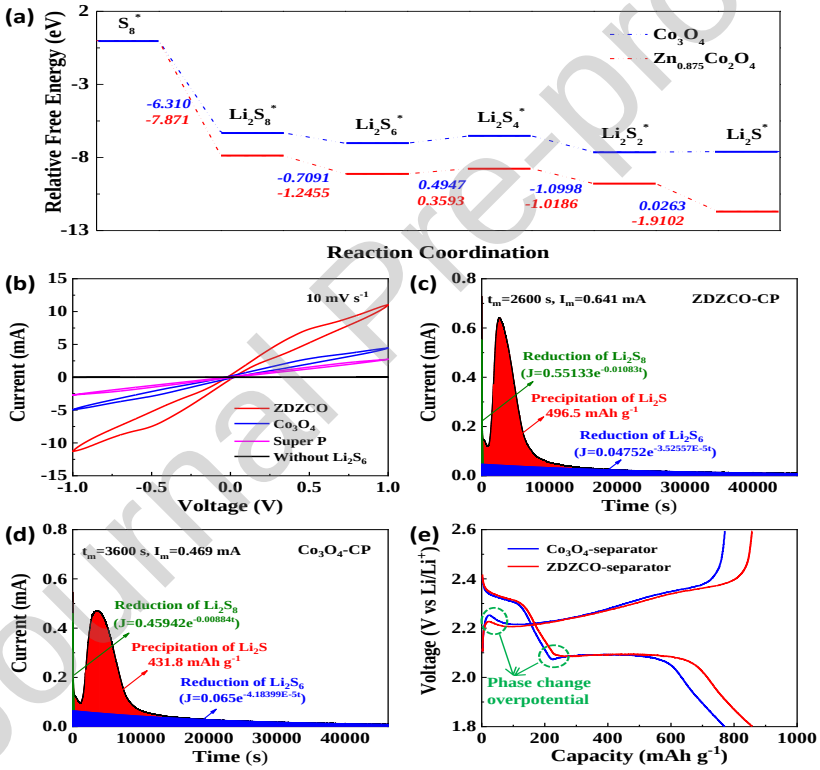

Figure 6. Catalytic effects of ZDZCO on polysulfide conversion: (a) The free energy diagrams for discharge process on the Co_3O_4 and $Zn_{0.875}Co_2O_4$ substrates, respectively; (b) CV curves of symmetric cells with ZDZCO, Co_3O_4, and super P electrodes; potentiostatic discharge curves of Li_2S precipitation experiments of (c) ZDZCO and (d) Co_3O_4 samples; (e) charge-discharge curves at the 125th cycle of the Li-S batteries with ZDZCO-separator and Co_3O_4-separator.

The second mechanism by which the performance is improved by the ZDZCO-separator is suspected to be through a catalytic effect for the continual conversion of polysulfides. The first evidence of this is the high discharge capacity at 6 C, as shown in Fig. 4d. To further expand on this, the charge-discharge profiles under various C-rates are displayed in Fig. S10. Even at high current density of 6 C, the Li-S battery with the ZDZCO-separator still shows two well-defined discharge plateaus, suggesting fast reaction kinetics. Fig. S11 shows that a much smaller charge-transfer resistance for the Li-S battery with ZDZCO-separator after cycling is obtained, also indicating fast redox kinetics. To understand the reason for the improved reaction kinetics, the free energies involved in each pathway of sulfur reduction on the surface of Co_3O_4 and $Zn_{0.875}Co_2O_4$, respectively, were calculated. As shown in Fig. 6a, the Gibbs free energies for the reduction of S_8 to Li_2S_8, Li_2S_8 to Li_2S_6, and Li_2S_4 to Li_2S_2 on the surface of both Co_3O_4 and $Zn_{0.875}Co_2O_4$ are negative, signifying the fast kinetics. On both substrates, the step to form Li_2S_4 is endothermic, suggestive of the sluggish reaction kinetics. Fortunately, the Gibbs free energy is reduced from 0.4947 eV on the Co_3O_4 substrate to only 0.3593 eV on $Zn_{0.875}Co_2O_4$, indicating a superior catalytic ability of $Zn_{0.875}Co_2O_4$. Notably, on the Co_3O_4 substrate, the reduction of Li_2S_2 to Li_2S is nearly thermoneutral, while on $Zn_{0.875}Co_2O_4$ this step is exothermic with a significantly negative Gibbs free energy. To experimentally study the kinetics of polysulfide redox reactions, CV measurements using symmetric cells with Li_2S_6 electrolyte were carried out. Firstly, the negligible current density for the CV curve using ZDZCO-based electrode without Li_2S_6 in the electrolyte suggests that the ZDZCO is inactive between -1.0 and 1.0 V. As shown in Fig. 6b, with Li_2S_6 electrolyte, the cell using ZDZCO-based electrode exhibits the highest current density, highlighting the significantly enhanced redox kinetics and facile polysulfide conversion on ZDZCO surface [57,58]. Theoretically, three quarters of the capacity of a Li-S battery results

from the conversion from the Li_2S_4 intermediate to Li_2S. Therefore, it is of great importance to evaluate the catalytic capability of host materials in facilitating Li_2S electrodeposition [59]. Fig. 6c and d show the potentiostatic discharge curves at 2.05 V for the Li_2S precipitation experiments on the ZDZCO and Co_3O_4 samples, respectively, which follow the galvanostatic discharge at 0.226 mA to 2.06 V. As shown, the contributions of polysulfide (Li_2S_8/Li_2S_6) reduction and Li_2S precipitation are mathematically modeled and distinguished. Obviously, the ZDZCO sample possesses a higher activity towards Li_2S precipitation with a higher peak current density (0.641 vs 0.469 mA). Also, the peak current for the Li_2S precipitation occurs much earlier for the ZDZCO sample (2600s vs 3600s), suggesting a higher Li_2S electrodeposition effective rate constant combining nucleation and growth rate constant [59,60]. Calculated from the integral of the current, the capacity of Li_2S precipitation on the ZDZCO sample (496.5 mAh g^{-1}) is also higher than that on the Co_3O_4 sample (431.8 mAh g^{-1}), based on the weight of the sulfur in the catholyte. Owing to the strong affinity and high catalytic effect, ZDZCO can induce a large amount of Li_2S to electrodeposit uniformly on the surface, as shown in Fig. S12. Fig. S12 also clearly shows that Li-O bonds and S-O bonds form, indicating a strong chemisorption effect between Li_2S and ZDZCO, which agrees with the theoretical calculation. These results have powerfully demonstrated that ZDZCO can significantly accelerate the polysulfide conversation. As a consequence, the adsorbed polysulfides on ZDZCO can be rapidly converted and consumed, making the ZDZCO anchoring functional material work enduringly during prolonged cycling. This can be obviously indicated by the lower overpotential during the phase change between the soluble polysulfides and insoluble Li_2S_2/Li_2S in the charge and discharge processes at the 125th cycle for Li-S battery with ZDZCO-separator (Fig. 6e).

To achieve high practical energy density, high-loading sulfur electrodes are of great importance so that high areal capacity is delivered [61,62]. Herein, by simply using the as-prepared ZDZCO-separator, high-loading Li-S batteries were successfully achieved using the traditional blade coating technique. It should be mentioned that when the sulfur loading increases, the weight and thickness of the ZDZCO polysulfide-blocking layer are unaltered. As shown in

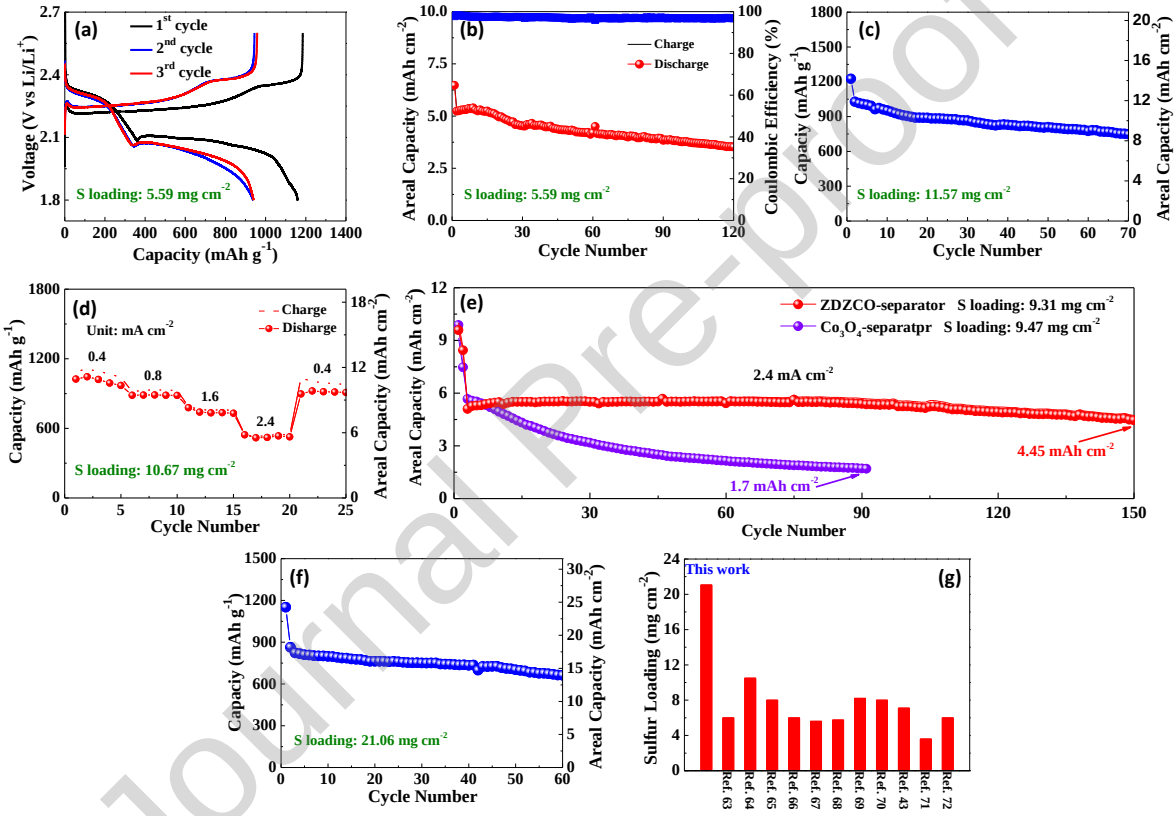

Figure 7. High loading Li-S batteries with ZDZCO-separator: (a) charge-discharge curves and (b) cycling performance with sulfur loading of 5.59 mg cm^{-2}; (c) cycling performance with sulfur loading of 11.57 mg cm^{-2}; (d) rate property with sulfur loading of 10.67 mg cm^{-2}; (e) long-term cycling performance at 2.4 mA cm^{-2} with sulfur loading of 9.31 mg cm^{-2}; (f) cycling performance with sulfur loading of 21.06 mg cm^{-2}; (g) comparison of the sulfur loading with recently excellent separator-related literature [43,63-72].

Fig. 7a, when the sulfur loading increases to 5.59 mg cm^{-2}, the as-obtained high-loading Li-S battery still shows typical electrochemical behavior of Li-S systems. Fig 7b displays that the high-loading Li-S battery can deliver an initial areal capacity of 6.47 mAh cm^{-2} at 0.3 mA cm^{-2}, which remains at 3.52 mAh cm^{-2} after 120 cycles at 1.2 mA cm^{-2}. It also should be noted that the high-loading battery possesses high coulombic efficiency (97.1% on average) during cycling, suggesting the suppressed shuttle effect. To exceed the state-of-the-art Li-ion batteries, the sulfur loading is further increased. Fig 7c shows that the Li-S battery with the loading of 11.57 mg cm^{-2} can give a capacity of 749 mAh g^{-1}, corresponding to an areal capacity of 8.66 mAh cm^{-2} after 70 cycles. Fig 7d and S13 indicate that the high-loading Li-S battery also shows excellent rate performance with a high capacity of 522 mAh g^{-1}, corresponding to 5.56 mAh cm^{-2} at 2.4 mA cm^{-2}. The long-term cycling test is also performed at a high current density of 2.4 mA cm^{-2}. It shows that the high-loading Li-S battery can stably cycle over 150 cycles with an areal capacity of 4.45 mAh cm^{-2} (Fig. 7e). However, the Li-S battery with the Co_3O_4-separator shows fast capacity fading with a low areal capacity of 1.7 mAh cm^{-2} after only 91 cycles. Furthermore, as displayed in Fig. S14, the Li-S battery with the Co_3O_4-separator suffers severely from the shuttle effect due to the insufficient binding and catalytic ability of Co_3O_4. Specially, in this study, Li-S batteries with a sulfur loading as high as 21.06 mg cm^{-2} can be successfully achieved under a low E/S ratio of ~12 μL mg^{-1}, which delivers an initial capacity of 1152 mAh g^{-1}, corresponding to 24.25 mAh cm^{-2}, and maintains a capacity of 663 mAh g^{-1}, corresponding to 13.95 mAh cm^{-2} after 60 cycles (Fig 7f). Fig 7g and Table S1 display that compared with the previously reported outstanding separator-related Li-S batteries, we obtained ultrahigh-loading Li-S batteries. Table S2 indicates that compared with recently published excellent literature using a traditional electrode preparation technique, our Li-S batteries can be operated under a comparable current

density with significantly extended cycling lifespan. To the best of our knowledge, such a cycling lifespan (over 210 days) of a Li-S battery with ultrahigh loading has rarely been reported. However, as shown in Fig. S15, due to the poor mechanical property of PVDF binder, large cracks occur in the thick sulfur electrode. We believe that in future study, through combining with robust binders, unique electrode configurations, high-performance anodes and electrolytes [33,73-76], our high-loading Li-S battery using ZDZCO-separator can possess high practical application potential. To visually demonstrate the high energy density of the as-prepared high-loading Li-S cells, we used a Li-S cell to power 12 LED lights. As displayed in Fig. S16, after 2h the LED lights are still sparkling, suggesting high energy density. Therefore, owing to the cation vacancies, the ZDZCO-separator can effectively anchor polysulfides and accelerate the redox kinetics, which significantly suppresses the shuttle effect and improves the electrochemical performance of high-loading Li-S battery for practical applications.

3. Conclusion

A bimetallic oxide with abundant cation vacancies has been prepared and applied to construct a multifunctional polysulfide-blocking layer on a separator for high-performance Li-S batteries. The cation vacancies can effectively boost the anchoring and catalytic effects of the multifunctional polysulfide-blocking layer, which have been powerfully proven via both theoretical and experimental studies. As a result, the multifunctional polysulfide-blocking layer on the separator can function as an upper current collector, polysulfide anchor, and catalytic reactor to significantly suppress the shuttle effect. Therefore, high-loading Li-S batteries can be successfully achieved by using the multifunctional polysulfide-blocking layer modified separator. Specially, Li-S battery with an ultrahigh loading of 21.06 mg cm^{-2} can be achieved, which can stably cycle over 60 cycles with a high areal capacity of 13.95 mAh cm^{-2}. This study offers an

effective and promising strategy to construct high-energy-density Li-S batteries with high loading.

Conflict of Interest

The authors declare no competing financial interest.

Acknowledgment

This work was supported by the National Natural Science Foundation of China (51802171, 22005169), the Taishan Scholars Program, Natural Science Foundation of Shandong Province, China (ZR2018BB031, ZR2020QB121), Youth Innovation of Shandong Higher Education Institutions, China (2019KJC004), Outstanding Youth Foundation of Shandong Province, China (ZR2019JQ14), the Applied Research Project for Postdoctoral Researcher of Qingdao City, China.

References

[1] M. Jiang, Z. Zhang, B. Tang, T. Dong, H. Xu, H. Zhang, X. Lu, G. Cui, Polymer electrolytes for Li-S batteries: Polymeric fundamentals and performance optimization, J. Energy Chem. 58 (2021) 300-317.

[2] Z. Li, S. Jiao, D. Yu, Q. Zhang, K. Liu, J. Han, Z. Guo, J. Liu, L. Wang, Cationic-polymer-functionalized separator as a high-efficiency polysulfide shuttle barrier for long-life Li-S battery, ACS Appl. Energy Mater. 4 (2021) 2914-2921.

[3] H. Du, S. Li, H. Qu, B. Lu, X. Wang, J. Chai, H. Zhang, J. Ma, Z. Zhang, G. Cui, Stable cycling of lithium-sulfur battery enabled by a reliable gel polymer electrolyte rich in ester groups, J. Membrane Sci. 550 (2018) 399-406.

[4] J. Liu, M. Sun, Q. Zhang, F. Dong, P. Kaghazchi, Y. Fang, S. Zhang, Z. Lin, A robust network binder with dual functions of Cu^{2+} ions as ionic crosslinking and chemical binding agents for highly stable Li-S batteries, J. Mater. Chem. A 6 (2018) 7382-7388.

[5] G. Hu, C. Xu, Z. Sun, S. Wang, H.M. Cheng, F. Li, W. Ren, 3D graphene-foam-reduced-graphene-oxide hybrid nested hierarchical networks for high-performance Li-S batteries, Adv. Mater. 28 (2016) 1603-1609.

[6] H. Qu, J. Ju, B. Chen, N. Xue, H. Du, X. Han, J. Zhang, G. Xu, Z. Yu, X. Wang, G. Cui, Inorganic separators enable significantly suppressed polysulfide shuttling in high-performance lithium-sulfur batteries, J. Mater. Chem. A 6 (2018) 23720-23729.

[7] T.Z. Hou, W.T. Xu, X. Chen, H.J. Peng, J.Q. Huang, Q. Zhang, Lithium bond chemistry in lithium-sulfur batteries, Angew. Chem. Int. Ed. 56 (2017) 8178-8182.

[8] S.S. Zhang, J.A. Read, A new direction for the performance improvement of rechargeable lithium/sulfur batteries, J. Power Sources 200 (2012) 77-82.

[9] J. Liang, Z.H. Sun, F. Li, H.M. Cheng, Carbon materials for Li-S batteries: Functional evolution and performance improvement, Energy Storage Mater. 2 (2016) 76-106.

[10] H. Du, Z. Zhang, J. He, Z. Cui, J. Chai, J. Ma, Z. Yang, C. Huang, G. Cui, A delicately designed sulfide graphdiyne compatible cathode for high-performance lithium/magnesium-sulfur batteries, Small 13 (2017) 1702277.

[11] L. Ma, H.L. Zhuang, S. Wei, K.E. Hendrickson, M.S. Kim, G. Cohn, R.G. Hennig, L.A. Archer, Enhanced Li-S batteries using amine-functionalized carbon nanotubes in the cathode, ACS Nano 10 (2016) 1050-1059.

[12] K. Park, J.H. Cho, J.H. Jang, B.C. Yu, A.T.D.L. Hoz, K.M. Miller, C.J. Ellison, J.B. Goodenough, Trapping lithium polysulfides of a Li-S battery by forming lithium bonds in a polymer matrix, Energy Environ. Sci. 8 (2015) 2389-2395.

[13] W. Chen, T. Qian, J. Xiong, N. Xu, X. Liu, J. Liu, J. Zhou, X. Shen, T. Yang, Y. Chen, C. Yan, A new type of multifunctional polar binder: Toward practical application of high energy lithium sulfur batteries, Adv. Mater. 29 (2017) 1605160.

[14] J. Liu, Y. Li, Y. Xuan, L. Zhou, D. Wang, Z. Li, H. Lin, S. Tretiak, H. Wang, L. Wang, Z. Guo, S. Zhang, Multifunctional cellulose nanocrystals as a high-efficient polysulfide stopper for practical Li-S batteries, ACS Appl. Mater. Interfaces 12 (2020) 17592-17601.

[15] H. Yang, J. Chen, J. Yang, Y. Nuli, J. Wang, Dense and high loading sulfurized pyrolyzed poly (acrylonitrile)(S@pPAN) cathode for rechargeable lithium batteries, Energy Stor. Mater. 31 (2020) 187-194.

[16] Y. Tian, G. Li, Y. Zhang, D. Luo, X. Wang, Y. Zhao, H. Liu, P. Ji, X. Du, J. Li, Z. Chen, Low-bandgap Se-deficient antimony selenide as a multifunctional polysulfide barrier toward high-performance lithium-sulfur batteries, Adv. Mater. 32 (2020) 1904876.

[17] X. Liang, L.F. Nazar, In situ reactive assembly of scalable core-shell sulfur-MnO_2 composite cathodes, ACS Nano 10 (2016) 4192-4198.

[18] K. Xi, D. He, C. Harris, Y. Wang, C. Lai, H. Li, P.R. Coxon, S. Ding, C. Wang, R.V. Kumar, Enhanced sulfur transformation by multifunctional FeS_2/FeS/S composites for high-volumetric capacity cathodes in lithium-sulfur batteries, Adv. Sci. 6 (2019) 1800815.

[19] Q. Sun, B. Xi, J.Y. Li, H. Mao, X. Ma, J. Liang, J. Feng, S. Xiong, Nitrogen-doped graphene-supported mixed transition-metal oxide porous particles to confine polysulfides for lithium-sulfur batteries, Adv. Energy Mater. 8 (2018) 1800595.

[20] D. Guo, F. Ming, H. Su, Y. Wu, W. Wahyudi, M. Li, M.N. Hedhili, G. Sheng, L.J. Li, H.N. Alshareef, Y. Li, Z. Lai, MXene based self-assembled cathode and antifouling separator for high-rate and dendrite-inhibited Li-S battery, Nano Energy 61 (2019) 478-485.

[21] J.Q. Huang, Q. Zhang, H.J. Peng, X.Y. Liu, W.Z. Qian, F. Wei, Ionic shield for polysulfides towards highly-stable lithium-sulfur batteries, Energy Environ. Sci. 7 (2014) 347-353.

[22] I. Bauer, S. Thieme, J. Brückner, H. Althues, S. Kaskel, Reduced polysulfide shuttle in lithium-sulfur batteries using nafion-based separators, J. Power Sources 251 (2014) 417-422.

[23] S.H. Chung, A. Manthiram, Bifunctional separator with a light-weight carbon-coating for dynamically and statically stable lithium-sulfur batteries, Adv. Funct. Mater. 24 (2014) 5299-5306.

[24] J.Q. Huang, Q. Zhang, F. Wei, Multi-functional separator/interlayer system for high-stable lithium-sulfur batteries: Progress and prospects, Energy Stor. Mater. 1 (2015) 127-145.

[25] C. Chen, Q. Jiang, H. Xu, Y. Zhang, B. Zhang, Z. Zhang, Z. Lin, S. Zhang, Ni/SiO_2/graphene-modified separator as a multifunctional polysulfide barrier for advanced lithium-sulfur batteries, Nano Energy 76 (2020) 105033.

[26] H. Yao, K. Yan, W. Li, G. Zheng, D. Kong, Z.W. Seh, V.K. Narasimhan, Z. Liang, Y. Cui, Improved lithium-sulfur batteries with a conductive coating on the separator to prevent the accumulation of inactive S-related species at the cathode-separator interface, Energy Environ. Sci. 7 (2014) 3381-3390.

[27] X. Gu, C. Tong, C. Lai, J. Qiu, X. Huang, W. Yang, B. Wen, L. Liu, Y. Hou, S. Zhang, A porous nitrogen and phosphorous dual doped graphene blocking layer for high performance Li-S batteries, J. Mater. Chem. A 3 (2015) 16670-16678.

[28] Y. Hu, X. Zhu, L. Wang, Two-dimensional material-functionalized separators for high-energy-density metal-sulfur and metal-based batteries, ChemSusChem 13 (2020) 1366-1378.

[29] S. Bai, X. Liu, K. Zhu, S. Wu, H. Zhou, Metal-organic framework-based separator for lithium-sulfur batteries, Nat. Energy 1 (2016) 16094.

[30] Y.X. Mo, J.X. Lin, Y.J. Wu, Z.W. Yin, Y.Q. Lu, J.T. Li, Y. Zhou, T. Sheng, L. Huang, S.G. Sun, Core-shell structured S@$Co(OH)_2$ with a carbon-nanofiber interlayer: A conductive cathode with suppressed shuttling effect for high-performance lithium-sulfur batteries, ACS Appl. Mater. Interfaces 11 (2019) 4065-4073.

[31] T. Lei, W. Chen, W. Lv, J. Huang, J. Zhu, J. Chu, C. Yan, C. Wu, Y. Yan, W. He, J. Xiong, Y. Li, C. Yan, J.B Goodenough. X. Duan, Inhibiting polysulfide shuttling with a graphene composite separator for highly robust lithium-sulfur batteries, Joule 2 (2018) 2091-2104.

[32] Z.A. Ghazi, X. He, A.M. Khattak, N.A. Khan, B. Liang, A. Iqbal, J. Wang, H. Sin, L. Li, Z. Tang, MoS_2/celgard separator as efficient polysulfide barrier for long-life lithium-sulfur batteries, Adv. Mater. 29 (2017) 1606817.

[33] J. Liu, D.G.D. Galpaya, L. Yan, M. Sun, Z. Lin, C. Yan, C. Liang, S. Zhang, Exploiting a robust biopolymer network binder for an ultrahigh-areal-capacity Li-S battery, Energy Environ. Sci. 10 (2017) 750-755.

[34] X. Wang, T. Gao, F. Han, Z. Ma, Z. Zhang, J. Li, C. Wang, Stabilizing high sulfur loading Li-S batteries by chemisorption of polysulfide on three-dimensional current collector, Nano Energy 30 (2016) 700-708.

[35] Y. Hu, W. Chen, T. Lei, Y. Jiao, J. Huang, A. Hu, C. Gong, C. Yan, X. Wang, J. Xiong, Strategies toward high-loading lithium-sulfur battery, Adv. Energy Mater. 10 (2020) 2000082.

[36] G. Zhou, S. Zhao, T. Wang, S.Z. Yang, B. Johannessen, H. Chen, C. Liu, Y. Ye, Y. Wu, Y. Peng, C. Liu, S.P. Jiang, Q. Zhang, Y. Cui, Theoretical calculation guided design of single-atom catalysts toward fast kinetic and long-life Li-S batteries, Nano Lett. 20 (2020) 1252-1261.

[37] Y. Song, W. Cai, L. Kong, J. Cai, Q. Zhang, J. Sun, Rationalizing electrocatalysis of Li-S chemistry by mediator design: Progress and prospects. Adv. Energy Mater. 10 (2020) 1901075.

[38] Z. Du, X. Chen, W. Hu, C. Chuang, S. Xie, A. Hu, W. Yan, X. Kong, X. Wu, H. Ji, L.J. Wan, Cobalt in nitrogen-doped graphene as single-atom catalyst for high-sulfur content lithium-sulfur batteries, J. Am. Chem. Soc. 141 (2019) 3977-3985.

[39] D. Liu, C. Zhang, G. Zhou, W. Lv, G. Ling, L. Zhi, Q.H. Yang, Catalytic effects in lithium-sulfur batteries: Promoted sulfur transformation and reduced shuttle effect, Adv. Sci. 5 (2018) 1700270.

[40] M. Yu, S. Zhou, Z. Wang, Y. Wang, N. Zhang, S. Wang, J. Zhao, J. Qiu, Accelerating polysulfide redox conversion on bifunctional electrocatalytic electrode for stable Li-S batteries, Energy Stor. Mater. 20 (2019) 98-107.

[41] D. Luo, G. Li, Y. Deng, Z. Zhang, J. Li, R. Liang, M. Li, Y. Jiang, W. Zhang, Y. Liu, W. Lei, A. Yu, Z. Chen, Synergistic engineering of defects and architecture in binary metal chalcogenide toward fast and reliable lithium-sulfur batteries, Adv. Energy Mater. 9 (2019) 1900228.

[42] W. Wang, Y. Zhao, Y. Zhang, J. Wang, G. Cui, M. Li, Z. Bakenov, X. Wang, Defect-rich multishelled Fe-doped Co_3O_4 hollow microspheres with multiple spatial confinements to

facilitate catalytic conversion of polysulfides for high-performance Li-S batteries, ACS Appl. Mater. Interfaces 12 (2020) 12763-12773.

[43] Z. Li, C. Zhou, J. Hua, X. Hong, C. Sun, H.W. Li, X. Xu, L. Mai, Engineering oxygen vacancies in a polysulfide-blocking layer with enhanced catalytic ability, Adv. Mater. 32 (2020) 1907444.

[44] H. Wu, H. Jiang, Y. Yang, C. Hou, H. Zhao, R. Xiao, H. Wang, Cobalt nitride nanoparticle coated hollow carbon spheres with nitrogen vacancies as an electrocatalyst for lithium-sulfur batteries, J. Mater. Chem. A 8 (2020) 14498-14505.

[45] Y. Li, X. Li, Y. Hao, A. Kakimov, D. Li, Q. Sun, L. Kou, Z. Tian, L. Shao, C. Zhang, J. Zhang, X. Sun, β-FeOOH interlayer with abundant oxygen vacancy toward boosting catalytic effect for lithium sulfur batteries, Front. Chem. 8 (2020) 309.

[46] Z. Chang, H. Dou, B. Ding, J. Wang, Y. Wang, X. Hao, D.R. MacFarlane, Co_3O_4 nanoneedle arrays as a multifunctional "super-reservoir" electrode for long cycle life Li-S batteries, J. Mater. Chem. A 5 (2017) 250-257.

[47] M. Carbone, Zn defective $ZnCo_2O_4$ nanorods as high capacity anode for lithium ion batteries, J. Electroanal. Chem. 815 (2018) 151-157.

[48] H. Kaftelen, K. Ocakoglu, R. Thomann, S. Tu, S. Weber, E. Erdem, EPR and photoluminescence spectroscopy studies on the defect structure of ZnO nanocrystals, Phys. Rev. B 86 (2012) 014113.

[49] J. Xu, W. Zhang, Y. Chen, H. Fan, D. Su, G. Wang, MOF-derived porous N-Co_3O_4@N-C nanododecahedra wrapped with reduced graphene oxide as a high capacity cathode for lithium-sulfur batteries, J. Mater. Chem. A 6 (2018) 2797-2807.

[50] S. S. Zhang, Role of $LiNO_3$ in rechargeable lithium/sulfur battery, Electrochim. Acta 70 (2012) 344-348.

[51] X. Ni, T. Qian, X. Liu, N. Xu, J. Liu, C. Yan, High lithium ion conductivity LiF/GO solid electrolyte interphase inhibiting the shuttle of lithium polysulfides in long-life Li-S batteries, Adv. Funct. Mater. 28 (2018) 1706513.

[52] H. Cheng, C.Y. Su, Z.Y. Tan, S.Z. Tai, Z.Q. Liu, Interacting $ZnCo_2O_4$ and Au nanodots on carbon nanotubes as highly efficient water oxidation eelectrocatalyst, J. Power Sources 357 (2017) 1-10.

[53] G. Huang, Y. Yang, H. Sun, S. Xu, J. Wang, M. Ahmad, Z. Xu, Defective $ZnCo_2O_4$ with Zn vacancies: Synthesis, property and electrochemical application, J. Alloy Compd. 724 (2017) 1149-1156.

[54] N. Joshi, L.F. da Silva, H.S. Jadhav, F.M. Shimizu, P.H. Suman, J.C. M'Peko, M.O. Orlandi, J.G. Seo, V.R. Mastelaro, O.N. Oliveira Jr, Yolk-shelled $ZnCo_2O_4$ microspheres: Surface properties and gas sensing application, Sensor Actuat. B-Chem. 257 (2018) 906-915.

[55] B. Liu, S. Huang, D. Kong, J. Hu, H.Y. Yang, Bifunctional $NiCo_2S_4$ catalysts supported on a carbon textile interlayer for ultra-stable Li-S battery, J. Mater. Chem. A 7 (2019) 7604-7613.

[56] Z. Ye, Y. Jiang, J. Qian, W. Li, T. Feng, L. Li, F. Wu, R. Chen, Exceptional adsorption and catalysis effects of hollow polyhedra/carbon nanotube confined CoP nanoparticles superstructures for enhanced lithium-sulfur batteries, Nano Energy 64 (2019) 103965.

[57] K. Shi, C. Lai, X. Liu, Y. Wei, W. Lv, J. Wang, J. Li, C. Yan, B. Li, Q.H. Yang, F. Kang, Y.B. He, $LiNi_{0.8}Co_{0.15}Al_{0.05}O_2$ as both a trapper and accelerator of polysulfides for lithium-sulfur batteries, Energy Storage Mater. 17 (2019) 111-117.

[58] D. An, L. Shen, D. Lei, L. Wang, H. Ye, B. Li, F. Kang, Y.B. He, An ultrathin and continuous $Li_4Ti_5O_{12}$ coated carbon nanofiber interlayer for high rate lithium sulfur battery, J. Energy Chem. 31 (2019) 19-26.

[59] Q. Wu, X. Zhou, J. Xu, F. Cao, C. Li, Adenine derivative host with interlaced 2D structure and dual lithiophilic-sulfiphilic sites to enable high-loading Li-S batteries, ACS Nano 13 (2019) 9520-9532.

[60] F.Y. Fan, W.C. Carter, Y.M. Chiang, Mechanism and kinetics of Li_2S precipitation in lithium-sulfur batteries, Adv. Mater. 27 (2015) 5203-5209.

[61] L. Wang, Y.B. He, L. Shen, D. Lei, J. Ma, H. Ye, K. Shi, B. Li, F. Kang, Ultra-small self-discharge and stable lithium-sulfur batteries achieved by synergetic effects of multicomponent sandwich-type composite interlayer, Nano Energy 50 (2018) 367-375.

[62] T. Liu, Q. Chu, C. Yan, S. Zhang, Z. Lin, J. Lu, Interweaving 3D network binder for high-areal-capacity Si anode through combined hard and soft polymers, Adv. Energy Mater. 9 (2019) 1802645.

[63] X.J. Hong, C.L. Song, Y. Yang, H.C. Tan, G.H. Li, Y.P. Cai, H. Wang, Cerium based metal-organic frameworks as an efficient separator coating catalyzing the conversion of polysulfides for high performance lithium-sulfur batteries, ACS Nano 13 (2019) 1923-1931.

[64] Z. Cheng, H. Pan, J. Chen, X. Meng, R. Wang, Separator modified by cobalt-embedded carbon nanosheets enabling chemisorption and catalytic effects of polysulfides for high-energy-density lithium-sulfur batteries, Adv. Energy Mater. 9 (2019) 1901609.

[65] Y. Zang, F. Pei, J. Huang, Z. Fu, G. Xu, X. Fang, Large-area preparation of crack-free crystalline microporous conductive membrane to upgrade high energy lithium-sulfur batteries, Adv. Energy Mater. 8 (2018) 1802052.

[66] X. Lv, T. Lei, B. Wang, W. Chen, Y. Jiao, Y. Hu, Y. Yan, J. Huang, J. Chu, C. Yan, C. Wu, J. Wang, X. Niu, J. Xiong, An efficient separator with low Li-ion diffusion energy barrier resolving feeble conductivity for practical lithium-sulfur batteries, Adv. Energy Mater. 9 (2019) 1901800.

[67] J. He, Y. Chen, A. Manthiram, Vertical Co_9S_8 hollow nanowall arrays grown on a celgard separator as a multifunctional polysulfide barrier for high-performance Li-S batteries, Energy Environ. Sci. 11 (2018) 2560-2568.

[68] D. Fang, Y. Wang, X. Liu, J. Yu, C. Qian, S. Chen, X. Wang, S. Zhang, Spider-web-inspired nanocomposite-modified separator: Structural and chemical cooperativity inhibiting the shuttle effect in Li-S batteries, ACS Nano 13 (2019) 1563-1573.

[69] G. Li, F. Lu, X. Dou, X. Wang, D. Luo, H. Sun, A. Yu, Z. Chen, Polysulfide regulation by the zwitterionic barrier toward durable lithium-sulfur batteries, J. Am. Chem. Soc. 142 (2020) 3583-3592.

[70] Z. Yu, B. Wang, X. Liao, K. Zhao, Z. Yang, F. Xia, C. Sun, Z. Wang, C. Fan, J. Zhang, Y. Wang, Boosting polysulfide redox kinetics by graphene-supported Ni nanoparticles with carbon coating, Adv. Energy Mater. 10 (2020) 2000907.

[71] J. Xie, B.Q. Li, H.J. Peng, Y.W. Song, M. Zhao, X. Chen, Q. Zhang, J.Q. Huang, Implanting atomic cobalt within mesoporous carbon toward highly stable lithium-sulfur batteries, Adv. Mater. 31 (2019) 1903813.

[72] L. Zhang, D. Liu, Z. Muhammad, F. Wan, W. Xie, Y. Wang, L. Song, Z. Niu, J. Chen, Single nickel atoms on nitrogen-doped graphene enabling enhanced kinetics of lithium-sulfur batteries, Adv. Mater. 31 (2019) 1903955.

[73] L. Qie, A. Manthiram, A facile layer-by-layer approach for high-areal-capacity sulfur cathodes, Adv. Mater. 27 (2015) 1694-1700.

[74] Z. Li, Y. Zhang, T. Liu, X. Gao, S. Li, M. Ling, C. Liang, J. Zheng, Z. Lin, Silicon anode with high initial coulombic efficiency by modulated trifunctional binder for high-areal-capacity lithium-ion batteries, Adv. Energy Mater. 10 (2020) 1903110.

[75] Z. Hu, S. Zhang, S. Dong, Q. Li, G. Cui, L. Chen, Self-stabilized solid electrolyte interface on a host-free Li-metal anode toward high areal capacity and rate utilization, Chem. Mater. 30 (2018) 4039-4047.

[76] J. Ju, S. Dong, Y. Cui, Y. Zhang, B. Tang, F. Jiang, Z. Cui, H. Zhang, X. Du, T. Lu, L. Huang, G. Cui, L. Chen, Leakage-proof electrolyte chemistry for a high-performance lithium-sulfur battery, https://doi.org/10.1002/anie.202103209.

Highlights

1. Cation-vacancy-rich bimetallic oxide constructs a novel multifunctional polysulfide-blocking layer.
2. Cation vacancies boost catalytic performance of the multifunctional polysulfide-blocking layer.
3. The Li-S battery achieves an ultrahigh loading of 21.06 mg cm^{-2} and prolonged lifespan of 60 cycles.

CRediT authorship contribution statement

Zhenwei Li, Luke Hencz: Experiment, Data collection and analysis, Writing. **Qian Zhang**: Theoretical study and analysis, Funding acquisition, Writing and review. **Jie Liu:** Conceptualization, Supervision, Funding acquisition, Writing and review. **Payam Kaghazchi**: Theoretical study, Writing-review & editing. **Jishu Han:** Resources. **Lei Wang:** Supervision, Resources, Funding acquisition. **Shanqing Zhang**: Conceptualization, Supervision, Writing-review & editing.

Declaration of interests

☒ The authors declare that they have no known competing financial interests or personal relationships that could have appeared to influence the work reported in this paper.

☐The authors declare the following financial interests/personal relationships which may be considered as potential competing interests: